The 2010 IEEE/RSJ International Conference on
Intelligent Robots and Systems
October 18-22, 2010, Taipei, Taiwan

Agile Turnaround Using Post-Stall Maneuvers for Tail-Sitter VTOL UAVs

Takaaki Matsumoto, Atsushi Konno, Ren Suzuki, Atsushi Oosedo, Kenta Go and Masaru Uchiyama

Abstract— **Miniature vertical take-off and landing unmanned aerial vehicles (VTOL UAVs) make various missions possible alone such as surveillance in partially-destroyed building and at broad hazard area where many obstacle exist. In such missions, agile turnaround using post-stall maneuvers is useful to avoid obstacles. This paper discusses agile turnaround strategies utilizing post-stall maneuvers for tail-sitter VTOL UAVs. Two agile turn strategies are studied in this paper: (1) minimum travel distance turn, and (2) minimum radius turn. The proposed strategies are formulated and optimization problems are solved. Through computer simulation, the proposed strategies are evaluated in terms of travel distance and turning radius comparing with conventional Immelmann turn strategy.**

I. INTRODUCTION

Thanks to electronic devices down-sizing, battery density growth and high-power motors, many small VTOL UAVs have been developed. Having both merits of fixed-wing and rotary-wing, miniature VTOL UAVs are expected to perform various missions, broad hazard area surveillance, indoor search and rescue, and launching at the rooftop of a building. There are several ways to perform VTOL maneuvers such as tilting-rotor, tilting-wing, thrust-vectoring and tail-sitting etc. As shown in Fig. 1, the simplest way is tail-sitting since it does not need extra actuators for the VTOL maneuver.

However, many tail-sitter UAVs have some complex equipments such as a coaxial contra-rotating propeller [1], a ducted fan and fins [2], side-by-side rotors [3],[4] and wingtip rotors [5] for the tail-sitting VTOL maneuver. Only few attempts have been made to develop tail-sitter UAVs without any extra equipments so far [6],[7],[8]. Although simple tail-sitter VTOL UAVs have only single rotor and conventional control surfaces (aileron, elevator and rudder), they have enough agility.

Historically, the agility capability of aircraft have been researched to execute post-stall combat maneuvers. Herbst have coined the term *supermaneuverability* and described example supermaneuver now commonly known as a Herbst maneuver ("J-turn") [9]. Having tactical positional advantage, the post-stall maneuvers have been demonstrated mainly by many supermaneuverable aircraft which have thrust vectoring and/or canard wing. Rockwell-MBB X-31 which has three-dimensional thrust vectoring performed some post-stall maneuvers [10]. Smith et al. have studied novel combat maneuvers through simulation with genetic algorithm [11].

This work was supported by Grant-in-Aid for Exploratory Research (No. 21656219), and JSPS Fellows (No. 216015).

Takaaki Matsumoto, Atsushi Konno, Ren Suzuki, Atsushi Oosedo, Kenta Go and Masaru Uchiyama are with Department of Aerospace Engineering, Tohoku University, Aoba-yama 6-6-01, Sendai 980-8579, Japan. takaaki@space.mech.tohoku.ac.jp

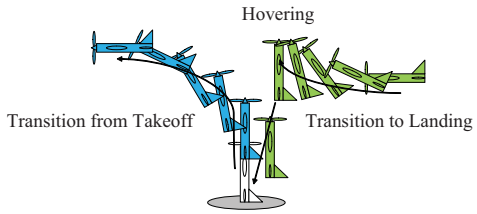

Fig. 1. Takeoff and landing of a tail-sitter VTOL aircraft.

The tail-sitter VTOL UAVs are not supermaneuverable, but its agility occupy an intermediate position between supermaneuverable aircrafts and conventional aircrafts. Since propeller slipstream generates aerodynamic forces to each control surfaces, the simple tail-sitter VTOL UAVs are able to control itself in post-stall condition. The combat maneuvers which realize tactical advantage are not necessary for todays miniature tail-sitter VTOL UAVs, however, the positional advantage of them still have utility value; for example, when it comes to surveillance in partially-destroyed building or at broad hazard area where many obstacle exist, minimal displacement maneuver can be useful.

There are several researches of optimal VTOL maneuver utilizing agility for tail-sitter VTOL UAVs, however, little work has been done to make use of agility to in-flight mission such as collision avoidance and flight in tight space. Stone et al. and Kubo et al. have studied stable time-optimal transition maneuvers between hovering and level flight for their tail-sitter VTOL UAVs in [3] and [4], however, their UAVs have complex equipments and other maneuvers which utilizes its agility were not discussed. From the aspect of collision avoidance path planning for normal UAVs, Richards et al. have proposed method for finding time-optimal trajectories for multiple aircraft avoiding collisions [12]. They demonstrated multiple waypoint path-planning for multiple aircraft, however, aircraft agility in post-stall condition were not utilized in [12]. Missile evasion maneuver of aircraft is pursuit-evasion problem and needs time optimality [13]. As for autonomous helicopter, Gavrilets et al. [14] and Abbeel et al. [15] have achieved various acrobatic maneuvers.

We have been developed simple tail-sitter UAV which is equipped with all necessary sensors and computers on the fuselage [16] and the stationary hovering, level and transition flight were achieved [17]. Integrating those flight mode, this paper discusses agile turnarounds using post-stall maneuver for tail-sitter VTOL UAVs. As typical agile turnarounds, two strategies: (1) minimum travel distance turn, and (2) minimum radius turn, are studied. Three-dimensional computer simulation are performed to verify the strategies. The

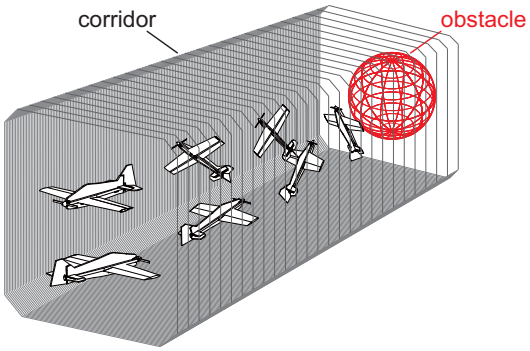

Fig. 2. Concept of indoor agile flight application.

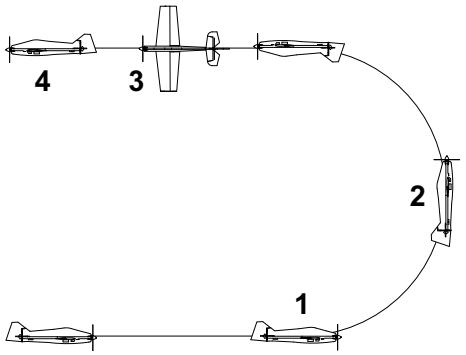

Fig. 3. Schematic view of conventional strategy: Immelmann turn.

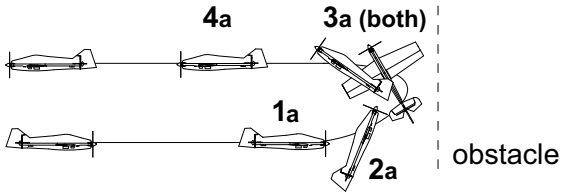

Fig. 4. Schematic view of the strategy A: minimum travel distance turn.

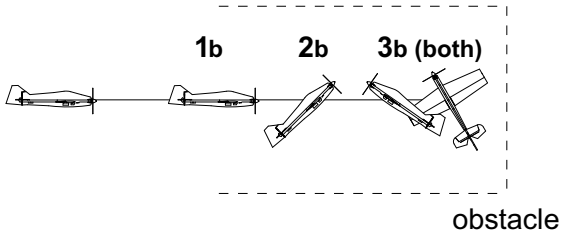

Fig. 7. Schematic view of the strategy B: minimum radius turn.

results of the two strategies are compared with results of the conventional Immelmann turn.

II. AGILE TURN MANEUVER

Generally, the desirable flight strategy of UAVs changes according to the situation. In case of quick turn to avoid collision in level flight, if UAVs are in high altitude, there are large space and no obstacle. UAVs can take various options and time-optimal flight strategy is suitable because need less time and energy. However, if the UAVs are in tight space, for example indoor or urban area where many obstacle exist, space-optimality of flight strategy is also important. Fig. 2 shows the concept of the space-optimal maneuver application.

A. Immelmann turn

There are some turnaround maneuvers for aircraft. One of the classic maneuver is the Immelmann turn. The Immelmann turn comprises following four steps:

Step 1. Level flight.
Step 2. Half loop.
Step 3. 180 ° roll to bring aircraft back level.
Step 4. Level flight (opposite direction).

Fig. 3 shows the concept of the Immelmann turn. The Immelmann turn is simple and stable maneuver which is executed in a sagittal plane. However, it needs large sagittal turning radius and relatively long time because it has half loop. If UAVs are in a tight space or do not have enough time to turn, such conventional maneuvers are not suitable to avoid obstacle.

B. Strategy A: Minimum travel distance turn

Fig. 4 shows the concept of the proposed minimum travel distance turn which achieves quick turn with minimum longitudinal travel distance, no lateral displacement and a little altitude gain. The proposed minimum travel distance turn comprises following four steps:

Step 1a. Level flight.
Step 2a. Pitch up to 100 ° with full throttle to brake the velocity.
Step 3a. Pitch down and throttle up to maximize braking force, then rolls 180 ° when velocity is almost zero.
Step 4a. Level flight (opposite direction).

At first, the aircraft keeps level flight. Then, the aircraft rises its pitch angle to over 90 ° (e.g. 100 °). In order to minimize the longitudinal travel distance, the acceleration along X direction should be minimized. There are two forces can be used to decrease its speed: the wind drag force and thrust force. If the pitch angle surpasses 90 ° , the thrust force affects to decelerate the aircraft. Hence the aircraft can use both wind drag and thrust forces to brake. However, the initial pitch angle is less than 90 ° because the aircraft is in level flight condition. If the aircraft rises its pitch angle with full throttle, its altitude increases while its pitch angle is less than 90 ° . In order to minimize the longitudinal travel distance, altitude constraint is relaxed until the pitch angle of aircraft reaches 90 ° in strategy A. In fact, the altitude change of strategy A is not very large because the time of Step 2a is very short.

After Step 2a, the pitch angle will surpass 90 ° but the aircraft will keep positive velocity for a while. The aircraft must keep the pitch angle and thrust force which generates maximum decelerating force.Therefore, Step 3a needs optimization calculation. In addition, the aircraft rolls 180 ° when its horizontal velocity is almost zero, because there are few drag and lift effects in such condition. In the rolling, reaction torque produced by propeller is utilized. When the aircraft gets large velocity, it reduces thrust force and returns to level flight (Step 4a) .

The two dimensional model of the UAV which have horizontal velocity is illustrated in Fig. 5. The two dimensional

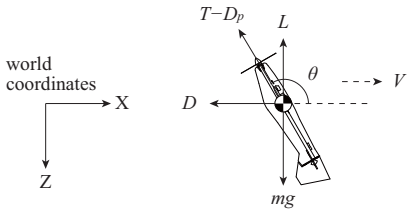

Fig. 5. Mathematical model and coordinates for optimization calculation.

optimization problem is given as follows,

$$\text{minimize} \quad \ddot{x}(n,\theta), \tag{1}$$

$$\text{subject to} \quad \begin{cases} \ddot{z} = 0, \\ n_{\min} \le n \le n_{\max}, \\ \frac{\pi}{2} \le \theta \le \pi. \end{cases} \tag{2}$$

where n is the propeller revolution speed, $n_{\min}$ is the 3000 rpm, $n_{\max}$ is the 7200 rpm and θ is pitch angle.

The translational dynamic equations of the UAV are

$$m\ddot{x} = (T - D_p)\cos\theta - D, \tag{3}$$

$$m\ddot{z} = -(T - D_p)\sin\theta - L + mg, \tag{4}$$

where m is the fuselage mass, T is the thrust force of the propeller, D_p is the drag force of propeller, θ is the pitch angle, D is the drag force, L is the lift force and g is the gravitational acceleration.

The aerodynamic forces are expressed as follows,

$$T = \rho n^2 {d_p}^4 C_T(u,n), \tag{5}$$

$$D_p = \frac{1}{2}\rho(V_p(n) - u)^2 A_b C_{D_p}, \tag{6}$$

$$L = \frac{1}{2}\rho V^2 S C_L(\alpha), \tag{7}$$

$$D = \frac{1}{2}\rho V^2 S C_D(\alpha), \tag{8}$$

where ρ is the air density, d_p is the diameter of propeller, C_T is the thrust coefficient of the motor and propeller, V_p is the velocity of propeller slipstream, u is the X directional velocity in the aircraft body coordinates, A_b is the projected area of the fuselage in propeller slipstream area, C_{Dp} is the drag coefficient of propeller, V is the aircraft translational velocity in the world coordinates, S is the main wing area, C_L is the lift coefficient, C_D is the drag coefficient and α is the angle of attack.

This optimization problem can be solved by SQP (Sequential Quadratic Programming). Using the technical computing language MATLAB (The MathWorks, Inc) and Optimization Toolbox, optimal pitch angle and propeller revolution speed are calculated for each velocity. Fig. 6 shows the results. The propeller revolution speed is maximum value and the pitch angle is monotone decreasing for all velocity range.

C. Strategy B: Minimum radius turn

As discussed in Section II-B, there is a relation of trade-off between restricting the altitude change during transition and minimizing the time when the pitch angle of aircraft is less than 90 ° . The strategy A tolerates such altitude changes,

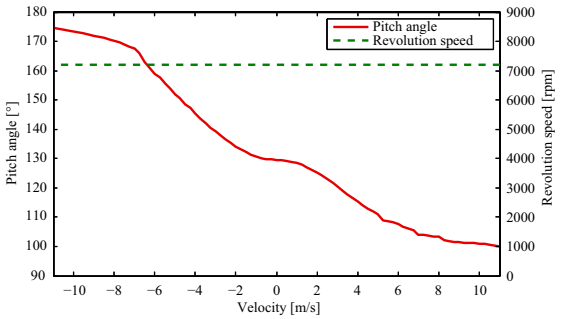

Fig. 6. Optimal pitch angle and propeller revolution speed for strategy A.

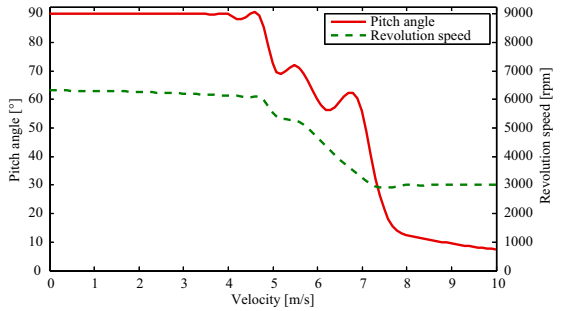

Fig. 8. Optimal pitch angle and propeller revolution speed for strategy B.

however, if altitude change is not allowed, strategy should be changed.

We propose another agile turnaround strategy in which altitude change is minimized (turning radius minimized). Fig. 7 shows the concept. The minimum radius turn comprises following steps:

Step 1b. Level flight.

Step 2b. Pitch up until near 90 ° and throttle down to keep altitude.

Step 3b. Pitch down and throttle up to maximize braking force and rolls 180 ° at velocity is almost zero.

Step 4b. Level flight (opposite direction).

Without the second step, the steps are the same as strategy A. In the Step 2b, keeping altitude, the aircraft rises its pitch angle to near 90 ° . In the beginning of Step 2b, the aircraft flies fast and can not take large pitch angle, because large pitch angle generates large lift force. To avoid this problem, the aircraft has to reduce propeller revolution speed to decrease its velocity. The optimization problem of this step is formulated as follows,

$$\text{minimize} \quad \ddot{x}(n,\theta), \tag{9}$$

$$\text{subject to} \quad \begin{cases} \ddot{z} = 0, \\ n_{min} \le n \le n_{max}, \\ 0 \le \theta \le \frac{\pi}{2}. \end{cases} \tag{10}$$

Fig. 8 shows the optimized profile of the pitch angle and propeller revolution speed. Since the propeller revolution speed reaches minimum value (3000 rpm), the pitch angle get smaller exponentially when the velocity exceeds 7.5 m/s. When the aircraft pitch angle is near 90 ° , Step 2b is terminated and Step 3b is started. The optimization problem of the Step 3b is the same as (1) and (2).

Fig. 9. Tail-Sitter UAV [17].

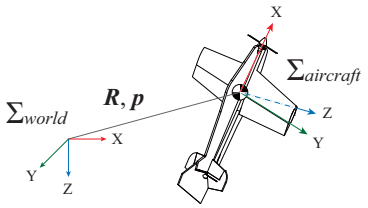

Fig. 10. World and aircraft body coordinates in the model.

III. SIMULATION

A. Simulation Model

A tail-sitter VTOL UAV [16] is shown in Fig. 9 . The main wingspan is 1.0 m, and the weight is 0.75 kg. The main and tail wings are parts of commercially available R/C airplane (Hyperion Co., Sniper 3D), and other parts such as the body are newly developed. The motor and propeller, of which the static thrust amounts to 120 % of the fuselage weight at a continuous maximum motor load are selected. The UAV is equipped with a microcomputer board, an attitude sensor, an inertial measurement unit, an ultrasonic sensor, a global positioning system receiver on the fuselage. In emergency, the UAV is controlled by human through a R/C receiver.

To evaluate the agile turn strategies, a three-dimensional tail-sitter UAV simulator was developed. Fig. 10 shows the world and aircraft coordinates in the model. The translational mathematical dynamic equation of the UAV in the aircraft body coordinates is represented as follows,

$$m(\dot{\boldsymbol{v}}+\boldsymbol{\omega}\times\boldsymbol{v}) = \boldsymbol{F}_B(\boldsymbol{v})+\boldsymbol{F}_S(\boldsymbol{v},\boldsymbol{\theta},n)+\boldsymbol{F}_P(\boldsymbol{v},n)+m\boldsymbol{R}^T\boldsymbol{g}, \tag{11}$$

where m is the fuselage mass, $\boldsymbol{v}$ is the translational velocity vector with respect to the aircraft body coordinates, $\boldsymbol{\theta}$ is the angle vector of control surface (aileron, elevator and rudder), n is the propeller revolution speed, $\boldsymbol{F}_B$ is the aircraft body aerodynamic force, $\boldsymbol{F}_S$ is the control surface aerodynamic force, $\boldsymbol{F}_P$ is the propeller thrust and drag force, $\boldsymbol{R}$ is the aircraft rotational matrix with respect to the world coordinates and $\boldsymbol{g}$ is the gravitational acceleration vector.

The rotational mathematical dynamic equation of the UAV in the aircraft body coordinates is represented as follows,

$$\boldsymbol{I}\dot{\boldsymbol{\omega}}+\boldsymbol{\omega}\times\boldsymbol{I}\boldsymbol{\omega} = \boldsymbol{M}_B(\boldsymbol{v})+\boldsymbol{M}_S(\boldsymbol{v},\boldsymbol{\theta},n)+\boldsymbol{M}_P(\boldsymbol{v},n)+\boldsymbol{C}(\boldsymbol{\omega}), \tag{12}$$

where $\boldsymbol{I}$ is the fuselage inertia tensor, $\boldsymbol{\omega}$ is the angular velocity vector around the aircraft body coordinates, $\boldsymbol{M}_B$ is the aircraft body aerodynamic moment, $\boldsymbol{M}_S$ is the control surface aerodynamic moment, $\boldsymbol{M}_P$ is the propeller torque and thrust moment and $\boldsymbol{C}$ is the inertial resistance.

Aerodynamic coefficients of main wing and fuselage are measured by experiments including wind tunnel test are performed with scale model of the UAV in all attitude. Inherent parameters of the propeller are measured through wind tunnel test. The momentum theory is used for propeller aerodynamic force calculation. Electrical and mechanical time constants of the DC motor are identified by experiment. The validity of simulator is confirmed by experiments.

B. Attitude Control

We proposed the optimal attitude transition which considers the hovering dynamics and achieves stable flight [18]. The optimal angular velocity around the aircraft body coordinates is

$$\boldsymbol{w}(t) = \sigma\boldsymbol{s}+\lambda\boldsymbol{l}. \tag{13}$$

where,

$$\int_0^1 \lambda dt = \Lambda, \tag{14}$$

$$\int_0^1 \sigma dt = \Sigma, \tag{15}$$

$$\cos\Lambda = \frac{\boldsymbol{F}\cdot\boldsymbol{R}_E\boldsymbol{F}}{\|\boldsymbol{F}\|\|\boldsymbol{R}_E\boldsymbol{F}\|}, \tag{16}$$

$$\cos\Sigma = \frac{\mathrm{Tr}(\boldsymbol{R}_L)-1}{2}, \tag{17}$$

$$\boldsymbol{l} = \begin{cases} \frac{\boldsymbol{F}\times\boldsymbol{R}_E\boldsymbol{F}}{\|\boldsymbol{F}\times\boldsymbol{R}_E\boldsymbol{F}\|}, & \text{for } \Lambda\neq 0 \\ \boldsymbol{0}, & \text{for } \Lambda = 0 \end{cases} \tag{18}$$

$$\hat{\boldsymbol{s}} = \frac{1}{2\sin\Sigma}\left(\boldsymbol{R}_L-\boldsymbol{R}_L^T\right), \tag{19}$$

$$\boldsymbol{R}_L = e^{-\Lambda\hat{\boldsymbol{l}}}\boldsymbol{R}_E, \tag{20}$$

$$\boldsymbol{R}_E = \boldsymbol{R}(t)^T\boldsymbol{R}_1, \tag{21}$$

where $\boldsymbol{F}$ is the thrust vector with respect to the aircraft coordinates. $\boldsymbol{R}(t)$ and $\boldsymbol{R}_1$ are the current and the reference aircraft rotational matrix with respect to the world coordinates, respectively. The trace of matrix Tr() is the sum of its diagonal entries and the hat operator transforms a vector into a skew symmetric matrix.

Each three axes of the aircraft are controlled by a PID controller. The control command is sent to control surfaces corresponding to each axis as follows:

$$\delta_i = -(K_P w_i + K_I\int w_i dt + K_D\dot{w}_i), \tag{22}$$

where δ_1, δ_2 and δ_3 are the aileron angle, elevator angle and rudder angle, respectively, and w_1, w_2 and w_3 are X, Y and Z components of axis-angle error between reference and current attitudes. The PID gains of level and hovering flight mode are determined by the ultimate sensitivity method, and tuned by trial and error. The gain values of intermediate mode between level and hovering flight are liner interpolated values. The gain values of real UAV are the same as those of simulation model.

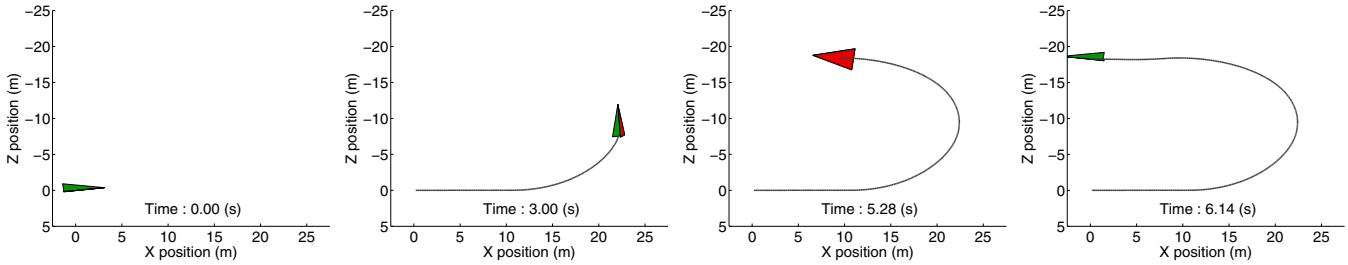

Fig. 11. Conventional Strategy: Immelman turn.

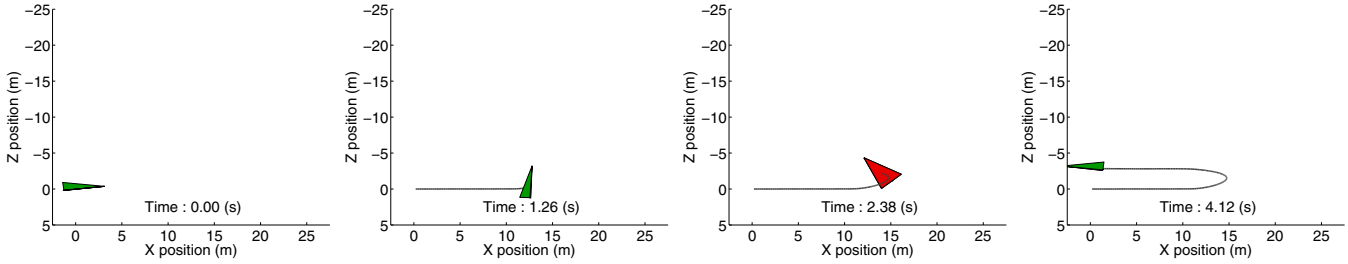

Fig. 12. Strategy A: Minimum travel distance turn.

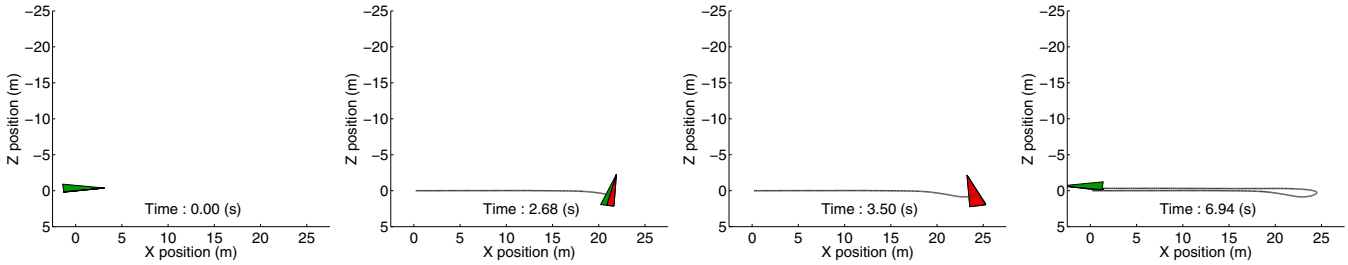

Fig. 13. Strategy B: Minimum radius turn.

C. Results

The computer simulations were practiced for each strategies. The initial condition is following: the aircraft starts flight at origin, the propeller revolution is 6000 rpm, the horizontal velocity is 10 m/s and the angle of attack is 7 ° . Each agile turnaround strategies are executed at 1 s after level flight. When the aircraft passes X origin again, the simulator determines that aircraft succeeded in turnaround, and finishes calculation.

1) Immelmann turn: Fig. 11 shows the movement with conventional strategy of the aircraft in sagittal plane. The radius of half loop was about 11 m. At 2.96 s, the aircraft pitch angle reached 90 ° but the Z directional velocity was approx 7 m/s. This speed was minimum value during the flight. The aircraft never stalled, however, large travel distance and radius were needed.

The attitude change during turnaround is shown in Fig. 14. All attitude were controlled successfully and there were no large error. Because propeller revolution speed kept maximum value, the aircraft velocity came to approx 12 m/s at the half loop, and 180 ° roll was finished in quite short time.

2) Strategy A (Minimum travel distance turn): Fig. 12 shows snapshots of one of the simulation with strategy A. The transition time and travel distance (X directional displacement) was shortest. The altitude change (Z directional displacement) was small enough. The attitude change is shown in Fig. 15. At 1.26 s, the aircraft pitch angle reached 90 ° . The step-like input contributes to shorten the Step 2a time as a result.

At 1.88 s, the aircraft started rolling because the velocity was less than 0.5 m/s. At 3.40 s, the aircraft velocity reached 10 m/s, so that the aircraft started level flight (Step 4a).

3) Strategy B (Minimum radius turn): Fig. 13 shows snapshots of one of the simulation with strategy B. Strategy B needed longest X directional displacement and transition time, but turn radius (Z directional displacement) was very much smaller than other two strategies. The attitude change is shown in Fig. 16.

Very long time was needed to finish Step 2b. It is difficult to shorten transition time while keeping altitude. In order to decrease flight velocity, the propeller revolution speed was reduced. However, it weaken pitching moment. At 2.68 s, the pitch angle reached 85 ° and Step 2b was terminated.

In the beginning of Step 3b, the translational velocity was almost zero and the aircraft started 180 ° rolling. Since the propeller revolution speed was reduced at Step 2b, the slipstream was weak and it needed long time to perform 180 ° roll. At 5.30 s, the aircraft velocity reached 10 m/s and the aircraft started level flight. Because the travel distance was longer than that of strategy A, the time of level flight

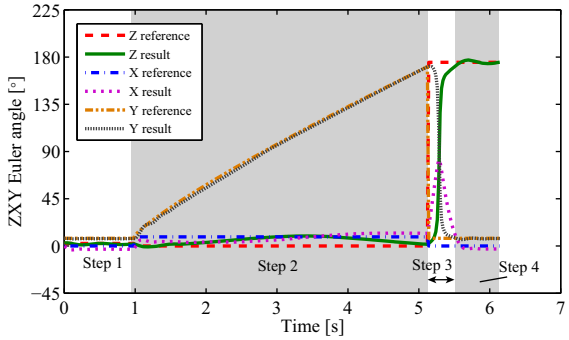

Fig. 14. Attitude change of Immelmann turn.

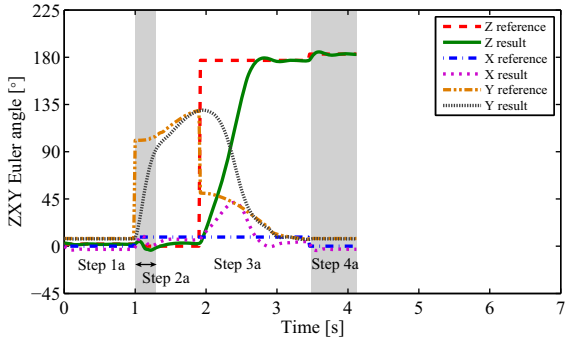

Fig. 15. Attitude change of strategy A.

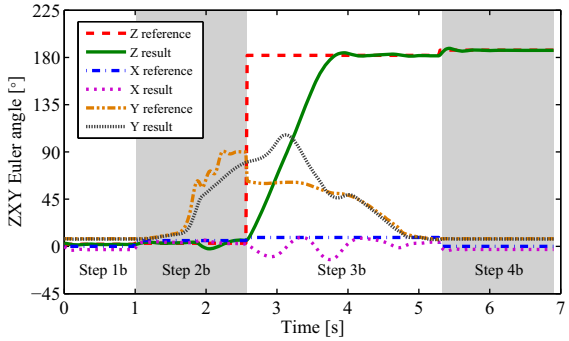

Fig. 16. Attitude change of strategy B.

TABLE I

SIMULATED DISPLACEMENT AND TRANSITION TIME.

Strategy	Immelmann	Strategy A	Strategy B
X [m]	12.12	**4.46**	14.22
Z [m]	18.41	2.84	**1.17**
Y [m]	0.40	0.50	0.70
Transition time [s]	6.14	**4.12**	6.94

was also longer.

4) Summary: The simulated displacements of each axes and transition time are shown in Table I. The strategy A needs the shortest transition time and travel distance (X directional displacement) of three strategies. The transition time and travel distance of strategy B are longer than that of conventional strategy, however, the turn radius (Z directional displacement) is less than 1 m and the smallest of three strategies. All strategies needed small lateral displacement. The purposes of proposed strategies are achieved completely.

IV. CONCLUSIONS

In this paper, we discussed the agile turnaround strategies utilizing post-stall maneuvers for tail-sitter VTOL UAVs. The proposed strategies were formulated into two dimensional optimization problems which were solved by SQP. The three-dimensional UAV simulator was developed to evaluate the strategy. The PID controller and attitude transition method [18] were implemented to the simulator. The proposed strategies were practiced through three-dimensional computer simulation and the results show that validity of proposed strategies. Flight experiment of the UAV with these proposed strategies will be reported in next paper.

REFERENCES

[1] T. Cord, Air Force Research Laboratory, Wright-Patterson AFB: "SkyTote Advanced Cargo Delivery System," *AIAA International Air and Space Symposium and Exposition: The Next 100 Years*, AIAA-2003-2753, 2003.

[2] C. Schaefer and L. Baskett: "GOLDENEYE: The Clandestine UAV," *2nd AIAA Unmanned Unlimited Systems, Technologies, and Operations*, AIAA-2003-6634, 2003.

[3] H. Stone and G. Clarke: "Optimization of Transition Maneuvers for a Tail-Sitter Unmanned Air Vehicle (UAV)," *in Proc. of the 2001 Australian International Aerospace Congress*, pp. 105, 2001.

[4] D. Kubo and S. Suzuki: "Tail-Sitter Vertical Takeoff and Landing Unmanned Aerial Vehicle: Transitional Flight Analysis," *J. of Aircraft*, vol. 45, no. 1, pp. 292-297, 2008.

[5] W. E. Green and P. Y. Oh: "Optic-Flow-Based Collision Avoidance - Applications Using a Hybrid MAV," *IEEE Robotics and Automation Magazine*, vol. 15, no. 1, pp. 96-103, 2008.

[6] A. Frank, J. S. McGrewy, M. Valentiz, D. Levinex and J. P. How:"Hover, Transition, and Level Flight Control Design for a Single-Propeller Indoor Airplane," *in Proc. of the 2007 AIAA Guidance, Navigation and Control Conference and Exhibit*, AIAA-2007-6318, 2007.

[7] N. B. Knoebel, T. W. McLain : "Adaptive Quaternion Control of a Miniature Tailsitter UAV," *in Proc. of the 2008 American Control Conference*, vol. 6, pp. 2340-2345, 2008.

[8] E. N. Johnson, A. Wu, J. C. Neidhoefer, S. K. Kannan and M. A. Turbe: "Flight-Test Results of Autonomous Airplane Transitions Between Steady-Level and Hovering Flight," *J. of Guidance, Control, and Dynamics*, vol. 31, no. 2, pp. 358-370, 2008.

[9] W. B. Herbst: "Future Fighter Technologies," *J. of Aircraft*, vol. 17, no. 8, pp. 561-566, 1980.

[10] C. W. Alcorn, M. A. Croom, M. S. Francis and H. Ross: "The X-31 aircraft: advances in aircraft agility and performance," *Progress in Aerospace Sciences*, vol. 32, no.4, pp 377-413, 1996.

[11] R.E. Smith, B.A. Dike, R.K. Mehra, B. Ravichandran, A. El-Fallah: "Classifier systems in combat: two-sided learning of maneuvers for advanced fighter aircraft," *Computer Methods in Applied Mechanics and Engineering*, vol. 186, no. 2-4, pp. 421-437, 2000.

[12] A. Richards, J. P. How: "Aircraft trajectory planning with collision avoidance using mixed integer linear programming," *in Proc. of the 2002 American Control Conference*, vol. 3, pp. 1936-1941, 2002.

[13] J. Karelahti, K. Virtanen, and T. Raivio: "Near-Optimal Missile Avoidance Trajectories via Receding Horizon Control," *J. of Guidance, Control, and Dynamics*, vol. 30, no. 5, 2007.

[14] V. Gavrilets, E. Frazzoli, B. Mettler, M. Piedmonte, and E. Feron: "Aggressive maneuvering of small autonomous helicopters: A human-centered approach," *The International Journal of Robotics Research*, vol. 20, no. 10, pp. 795-807, 2001.

[15] P. Abbeel, A. Coates, M. Quigley, and A. Ng: "An application of reinforcement learning to aerobatic helicopter flight," *in Proc. of the 2007 Advances in Neural Information Processing Systems*, 2007.

[16] K. Kita, A. Konno and M. Uchiyama: "Hovering Control of a Tail-Sitter VTOL Aerial Robot," *J. of Robotics and Mechatronics*, vol. 21, no. 2, pp. 277-283, 2009.

[17] K. Kita, A. Konno and M. Uchiyama: "Transitions Between Level-Flight and Hovering of a Tail-Sitter VTOL Aerial Robot," *Advanced Robotics*, vo. 24, no. 5-6, pp. 763-781, 2010.

[18] T. Matsumoto, K. Kita, R. Suzuki, A. Oosedo, K. Go, Y. Hoshino, A. Konno and M. Uchiyama: "A Hovering Control Strategy for a Tail-Sitter VTOL UAV that Increases Stability Against Large Disturbance," *in Proc. of the 2010 IEEE Int. Conf. of Robotics and Automation*, pp. 54-59, 2010.